

Supplementary Information

Multifunctional nanoagents for ultrasensitive imaging and photoactive killing of Gram-negative and Gram-positive bacteria

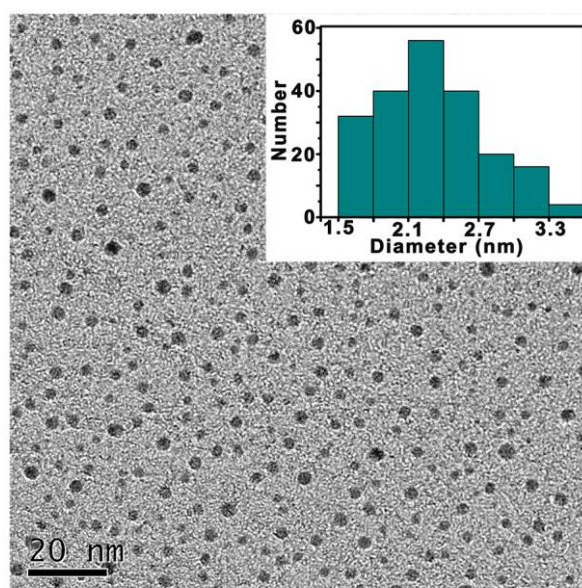
Jiali Tang,[‡] Binbin Chu,[‡] Jinhua Wang, Bin Song, Yuanyuan Su, Houyu Wang* & Yao He*

Laboratory of Nanoscale Biochemical Analysis, Institute of Functional Nano and Soft Materials (FUNSOM), Soochow University, Suzhou 215123, China

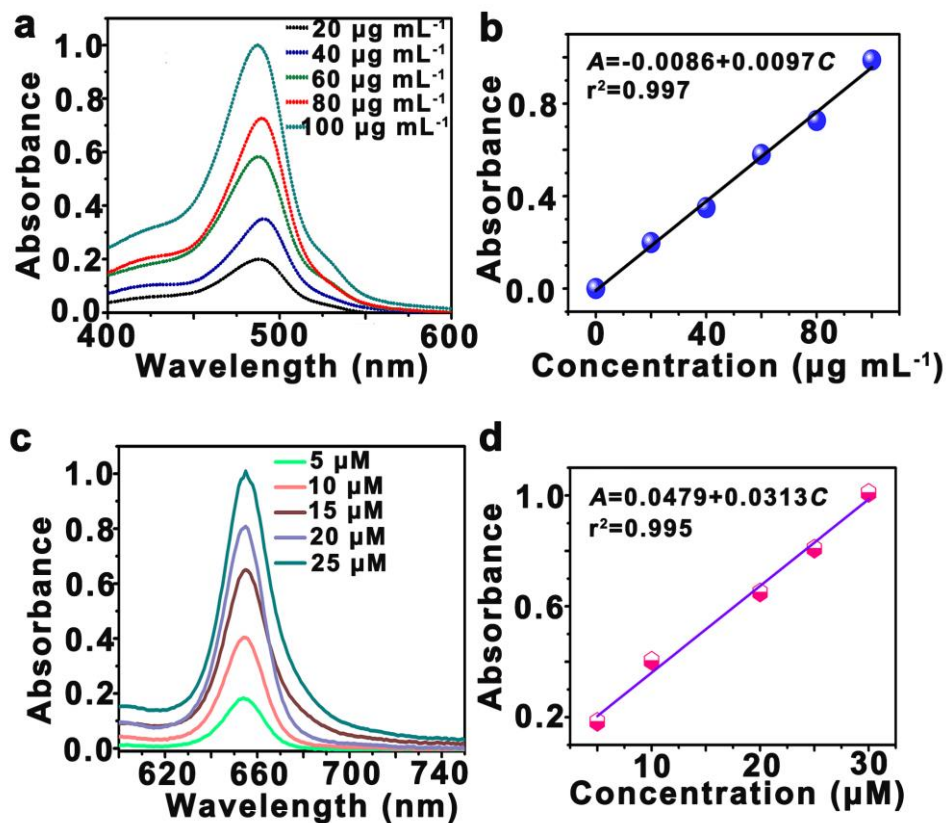
*Corresponding authors. Email: houyuwang@suda.edu.cn; yaohe@suda.edu.cn

[‡]These authors contributed equally to this work.

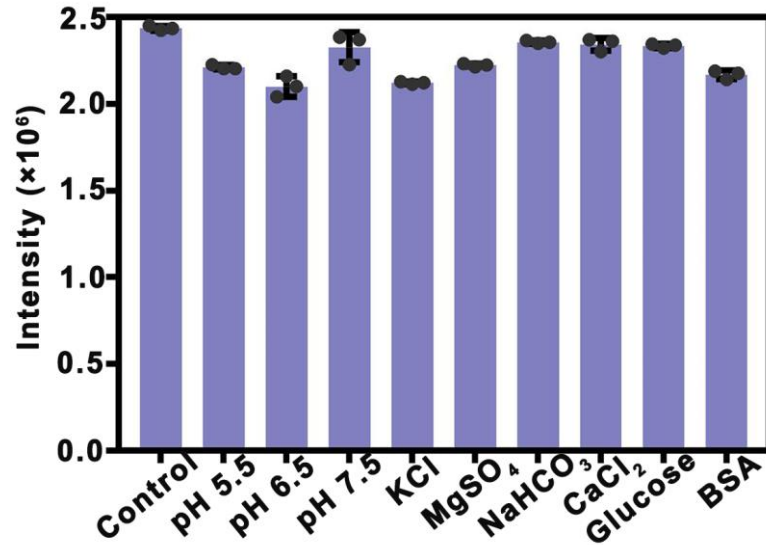
Supplementary Figures



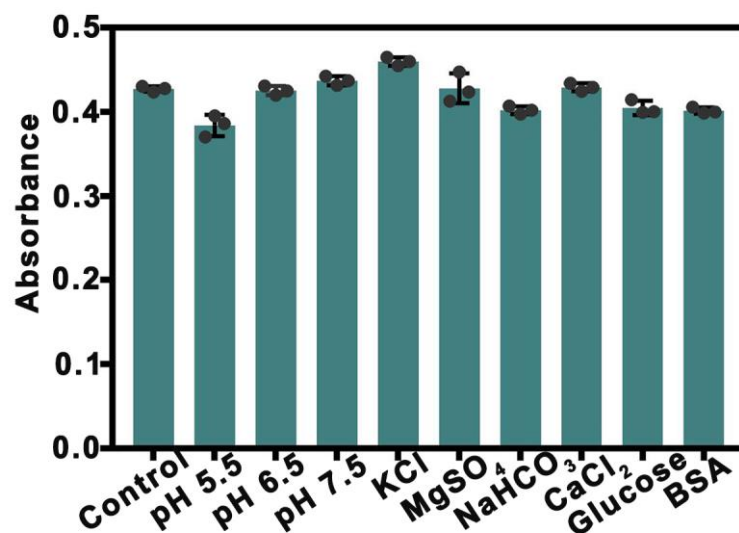
Supplementary Fig. 1. TEM image and corresponding size distribution of SiNPs (Inset). The average size of SiNPs is calculated by measuring over 200 particles. Scale bar: 20 nm.



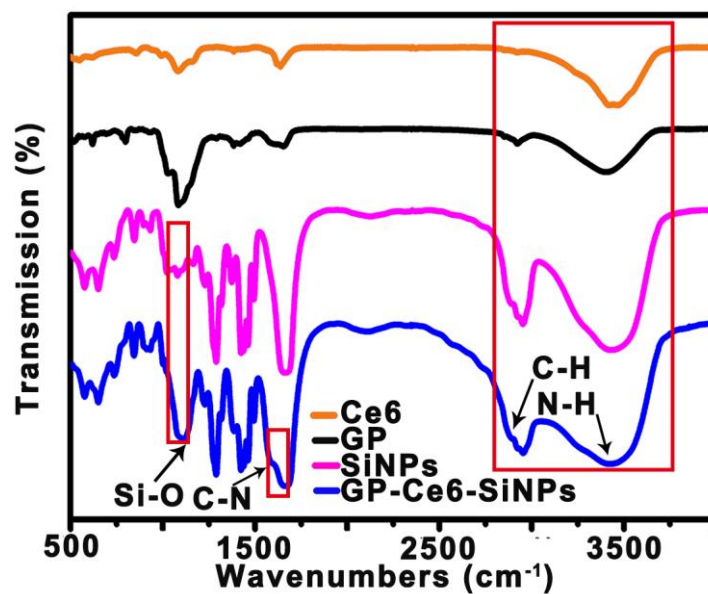
Supplementary Fig. 2. UV-vis absorption spectra of GP treated by phenol-sulfuric acid and UV-vis absorption spectra of Ce6. UV-vis absorption spectra of GP with various concentrations ranged from 20 to 100 $\mu\text{g mL}^{-1}$ treated by the same amount of phenol-sulfuric acid (a) and corresponding calibration curve (b). UV-vis absorption spectra of Ce6 with various concentrations ranged from 5 to 25 μM (c) and corresponding calibration curve (d). Source data are provided as a Source Data file.



Supplementary Fig. 3. Stability test of SiNPs in nanoagents. The intensity of SiNPs in nanoagents is tested in various kinds of solutions with different pH values (pH 5.5~7.5), as well as different kinds of solutions containing various intracellular species (e.g., 150 mM KCl, 2 mM MgSO₄, 10 mM NaHCO₃, 2 mM CaCl₂, 20 mM glucose, and 1 mM bovine serum albumin (BSA)). All error bars represent the standard deviation determined from three independent assays. Source data are provided as a Source Data file.

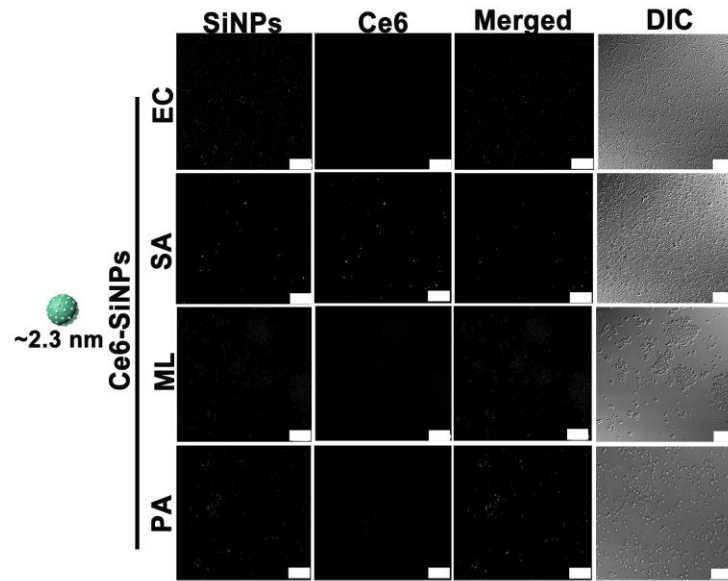


Supplementary Fig. 4. Stability test of Ce6 in nanoagents. The UV-vis absorbance value of Ce6 at 660 nm ($A_{660\text{nm}}$) in nanoagents in a series of solutions with different pH values (pH 5.5~7.5) and solutions containing various intracellular species (e.g., 150 mM KCl, 2 mM MgSO₄, 10 mM NaHCO₃, 2 mM CaCl₂, 20 mM glucose, and 1 mM BSA). All error bars represent the standard deviation determined from three independent assays. Source data are provided as a Source Data file.

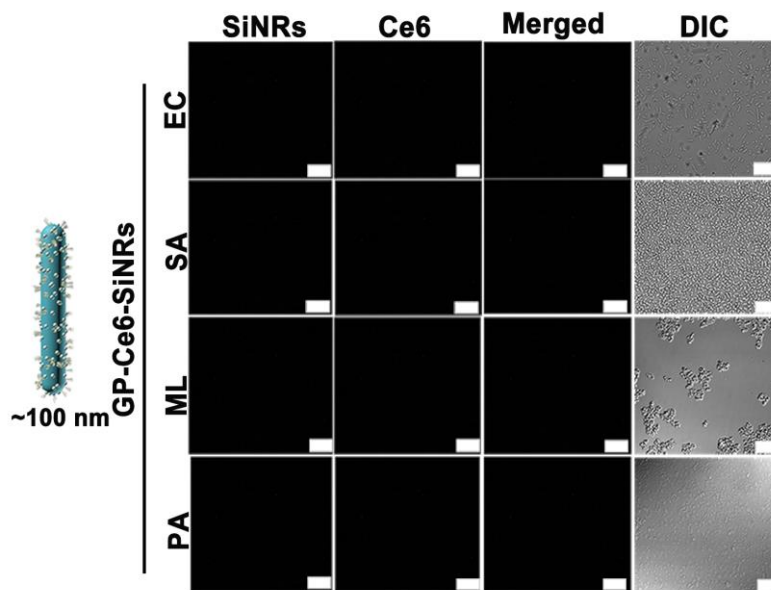


Supplementary Fig. 5. FTIR spectra of Ce6, GP, SiNPs and GP-Ce6-SiNPs.

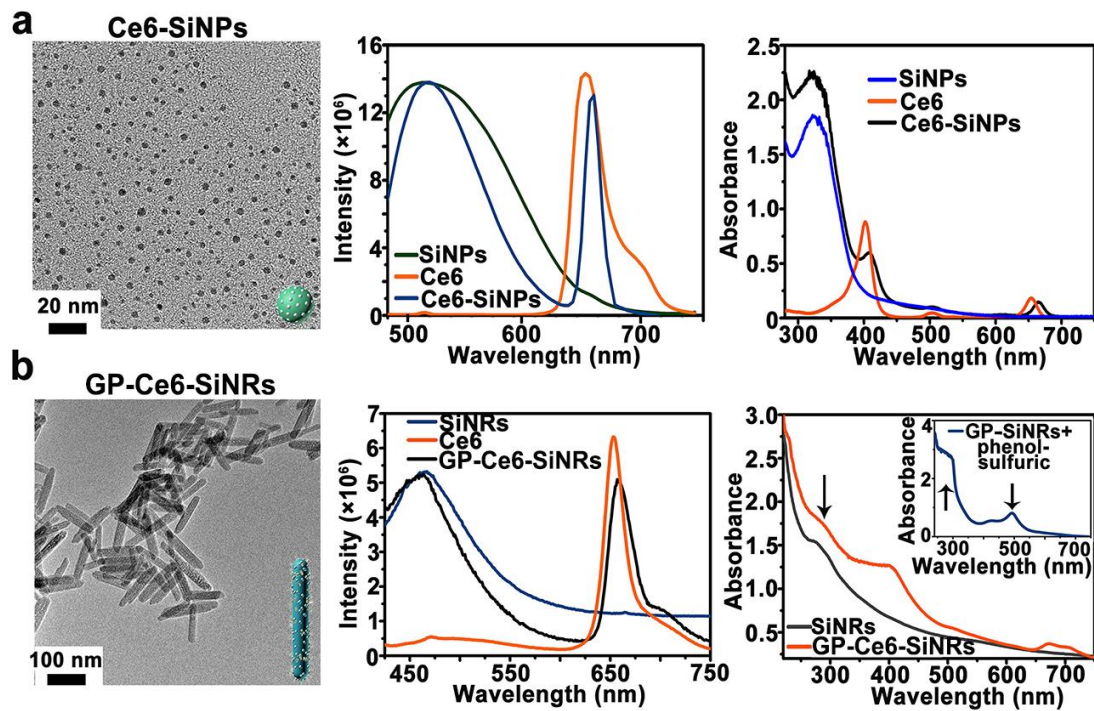
Source data are provided as a Source Data file.



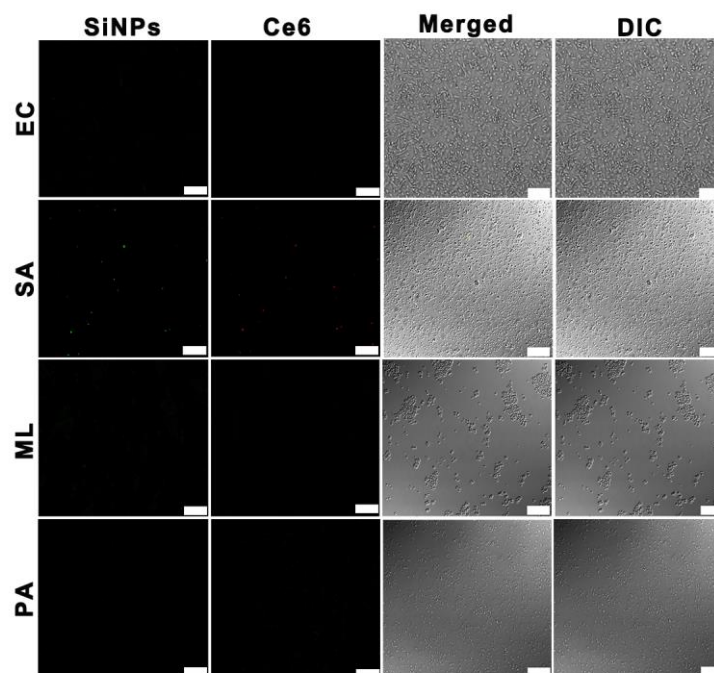
Supplementary Fig. 6. Confocal fluorescence images of bacteria (EC, SA, ML and PA) incubated with Ce6-SiNPs (10 mg mL^{-1}) without GP for 2 h. Scale bar: $10 \mu\text{m}$.



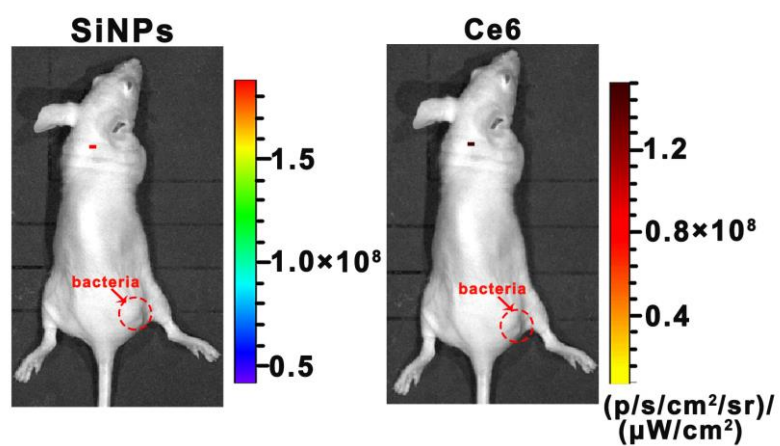
Supplementary Fig. 7. Confocal fluorescence images of bacteria (EC, SA, ML and PA) incubated with GP-Ce6-SiNRs (10 mg mL^{-1}) for 2 h. Scale bar: $10 \text{ }\mu\text{m}$.



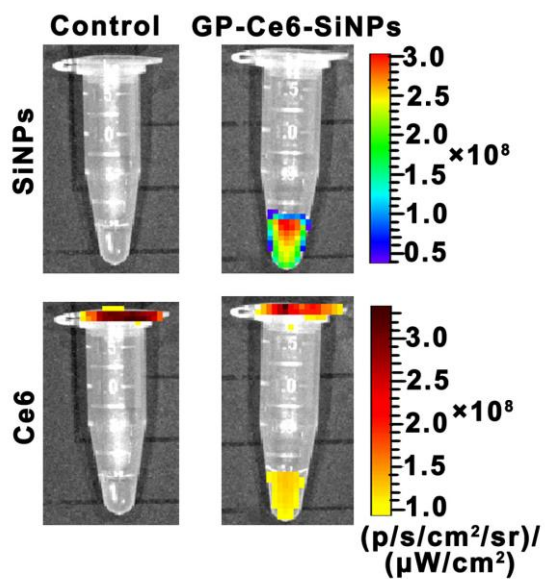
Supplementary Fig. 8. Characterizations (TEM images, PL spectra and UV-vis absorbance) of Ce6-SiNPs (a) and GP-Ce6-SiNRs (b), respectively. Source data are provided as a Source Data file.



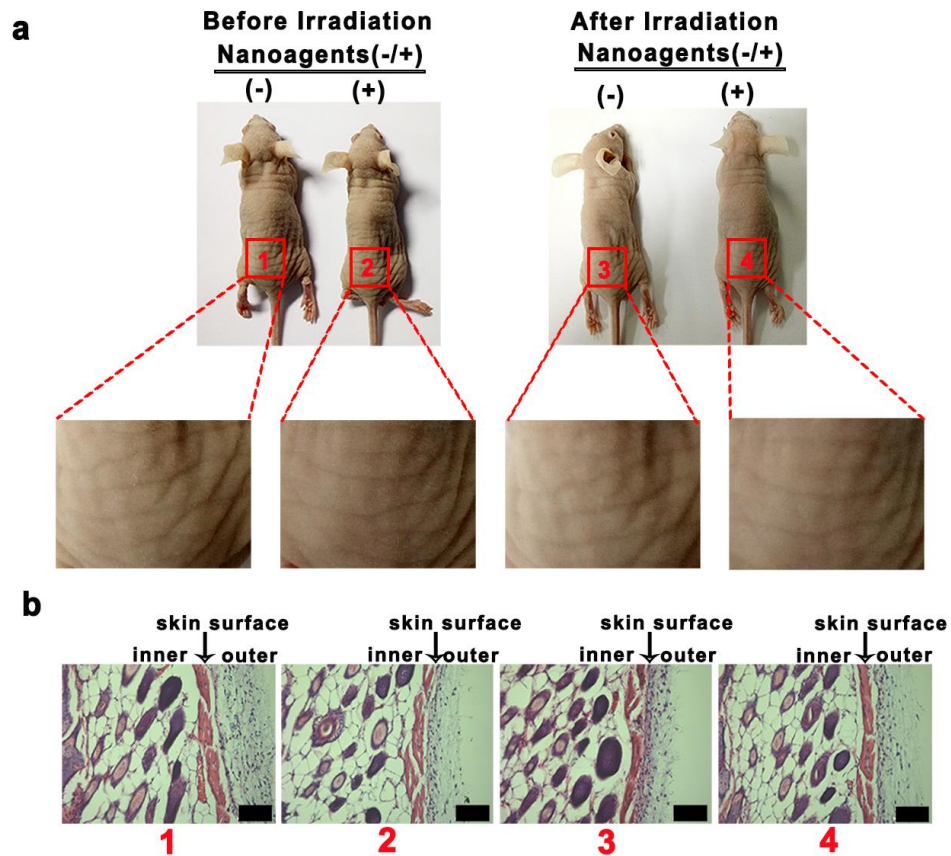
Supplementary Fig. 9. Confocal fluorescence images of four different kinds of bacteria (EC, SA, ML and PA) after incubation with GP-Ce6-SiNPs (10 mg mL^{-1}) for 2 h at $4 \text{ }^\circ\text{C}$. Scale bar: $10 \text{ }\mu\text{m}$.



Supplementary Fig. 10. *In vivo* imaging of SA (1.0×10^7 CFU)-infected mice treated with Ce6-SiNPs ($100 \mu\text{L}$, 10 mg mL^{-1}) at 24-h postinjection.



Supplementary Fig. 11. Urine signals from healthy mice treated without or with GP-Ce6-SiNPs after 4-h postinjection. Left: urine from mice treated without GP-Ce6-SiNPs. Right: urine from mice intravenously injected with GP-Ce6-SiNPs (100 μL , 10 mg mL^{-1}).



Supplementary Fig. 12. Assessment of toxicity of irradiation (660 nm, 12 mW cm⁻²) on skin. Photos (a) and the corresponding histological images (b) of skin tissues of healthy mice treated with or without nanoagents (100 μL, 10 mg mL⁻¹) before and after irradiation. Scale bar: 100 μm.

Supplementary Methods

The silicon nanorods (SiNRs) were synthesized based on the microwave-assisted approach¹. In details, the precursor solution was based on the addition of C₆H₁₇NO₃Si of 1 mL to N₂-saturated aqueous solution of 8 mL dispersed with 0.075 g of trisodium citrate. Then, the 10 mg of milk was mixed into the citric acid aqueous solution under constant stirring. The mixture was stirred for 15 min and then transferred into the 15 mL exclusive vitreous vessel. The SiNRs were prepared under 150 °C for 1 h. After microwave irradiation, the sample was collected when the temperature cooled to lower than 30 °C naturally. The residual reagents such as C₆H₁₇NO₃Si and trisodium citrate were removed by dialysis (1000 Da). Next, to further purify the as-prepared SiNRs, the obtained solution was centrifuged for 5 min at 8000 rpm, discarding the supernatant. The precipitate was re-dispersed in water and centrifuged again at 8000 rpm for 5 min. Such treatment repeated three times until the supernatant was transparent. Finally, the SiNRs were re-dispersed in water for further use.

To prepare GP-Ce6-SiNRs, the SiNRs solution (150 μL, 0.5 mg mL⁻¹) was mixed with GP dissolved in deionized water (150 μL, 10 mg mL⁻¹). The dispersion was continuously stirred at 70 °C for 6 h, and 0.01 mg of NaBH₄ was added and reacted for another 12 h at room temperature to obtain the stable GP modified SiNRs. To remove the unreacted GP, the reaction solution was filtered by using Nanosep centrifugal devices (MW cutoff, 3 kDa; Millipore) through centrifugation at 7500 rpm for 15 min. To further fabricate the GP-Ce6-SiNRs, the Ce6 solution (50 μL, 200 μM) was added in the above prepared GP-SiNRs solution and stirred at room temperature overnight. Then the excess free or unreacted Ce6 was removed using Nanosep centrifugal devices (MW cutoff, 3 kDa; Millipore) through centrifugation at 7000 rpm for 10 min. The final product was collected and stored at 4 °C in the dark for the following experiments.

Supplementary References

1. Song, B. *et al.* One-dimensional fluorescent silicon nanorods featuring ultrahigh photostability, favorable biocompatibility, and excitation wavelength-dependent emission spectra. *J. Am. Chem. Soc.* **138**, 4824-4831 (2016).